Geologic Structure of Western Primorye: Structuring Dynamics

P. L. Nevolin[a], V. P. Utkin[a], A. N. Mitrokhin[a], and T. K. Kutub-Zade[b, †]

[a] *Far East Geological Institute, Far East Branch, Russian Academy of Sciences,
pr. Stoletiya Vladivostoka 159, Vladivostok, 690022 Russia*
e-mail: stakhor@yandex.ru

[b]*Open Joint-Stock Company Primorgeologiya, Okeanskii pr. 29/31, Vladivostok, 690091 Russia*

Received August 20, 2011

Abstract—The first data are reported on the structuring dynamics of Western Primorye. The analysis of the structural parageneses of the least studied macro- and mesolevels of the arrangement of the geologic space allowed us to distinguish three sequentially superposed structural patterns (parageneses), each of which was formed by its own stress field during separate geodynamic periods: the Late Proterozoic–Early Paleozoic, the Middle–Late Paleozoic, and the Mesozoic–Cenozoic. During the first two episodes of geodynamic activation (Late Proterozoic–Early Paleozoic), the main compression axis was oriented longitudinally. The first episode was characterized by the formation of a thrust–fold structural pattern. The second episode resulted in the superposition of the meridional riftogenic structures and, respectively, in the pull-apart normal-fault segmentation of the crystalline basement into mainly longitudinal blocks, which partially coincide with the previously distinguished terranes. During the latitudinal compression and oblate deformation that predominanted during the Middle–Late Paleozoic geodynamic period, the down-thrown and uplifted blocks were transformed into depressions and arches, respectively. The depressions were filled with Paleozoic sediments, while the primary rocks in the arches experienced granitization with the formation of two granitic complexes that joined terranes. The granites are characterized by shadow and shear-type fold and pseudofolded forms. The Mesozoic–Cenozoic period governed by NNW compression is divided into the Triassic–Jurassic, Early Cretaceous, and Tertiary tectonic episodes. During the Triassic–Jurassic period, the ENE-trending narrow arches and depressions were formed by warping. The arches accumulated granitized rocks, while the depressions were compensated for by the Early–Late Triassic sedimentary–volcanogenic sediments. All these processes led to the formation of structural complexes that joined and overlapped older complexes of meridional blocks (terranes) across the strike. Two subsequent Mesozoic–Cenozoic episodes manifested themselves in the discrete formation of coal-bearing depressions due to the NNW compression and ENE extension of the warping products.

Keywords: structuring dynamics, structural parageneses, stress fields, geodynamic periods, Western Primorye, Far East

DOI: 10.1134/S1819714012040045

INTRODUCTION

Western Primorye has been studied for more than 50 years by many known geologists during the geological mapping and prospecting. In addition, Belyaevskii [3], Bersenev [4, 10], Vasil'kovskii, Gnibidenko [11], and many other researchers focused their attention on the geological structure of the territory. This resulted in the recognition of complexes of different genesis and wide age ranges (from the Riphean to the Cenozoic) and numerous metallogenic objects. The Laoelin–Grodekovo and Voznesenka terranes [34, 35] were recently distinguished instead of the previous Western Primorye and Grodekovo lithotectonic zones, respectively [13], which are partly in contact via the Western Primorye fault [4]. The Western Primorye zone or Laoelin–Grodekovo terrane are ascribed to the Jilin–

Laoelin fold system [16], which separates the Chinese shield and the Khanka Massif. The Grodekovo zone with the Voznesenka subzone represents the Khanka Massif margin, which is overlapped by Paleozoic sediments, and are combined into the Voznesensky terrane. Two approaches have been proposed to decipher the nature of the Khanka Massif [14]. One approach suggests that the Khanka Massif is a fragment of the Chinese Platform activated in the Silurian [14, 31, and others]. According to another approach, this massif is considered as the core of the continental growth [6, 11, 19, 21]. In spite of the fact that the discussion between the proponents of these two approaches and other less significant controversies were based on tectonic considerations, the results of structural observations usually were omitted.

The last data on the stratigraphy, magmatism, metallogeny, and geochronology of Western Primorye

---

[1] Deceased.

were obtained in the course of the additional geological study of the areas of sheets L-52-XXX and XXXVI on a scale of 1 : 200000 (GDP-200) (Kutub-Zade et al., 2010) (Figs. 1, 2). In this paper, we consider the structural evolution of this territory with focuses on the structural arrangement of the geologic space at the macro- and mesolevels. The micro- and megalevels were also distinguished. The microlevel is studied using a special apparatus. The macrolevel is observed in rocky exposures, while the mesolevel is deciphered in the large- and small-scaled maps of diverse geological specialization. The study of the megalevel is based on a system of global methods. Such a series of levels is consistent with the theoretical system of the structural arrangement of the lithosphere [8, 9].

The technique of our studies is based on the works of many researchers of structural-tectonic schools. The main methodical principle is the study of the structural patterns and parageneses representing direct dynamic indicators [7, 20]. Following [7, 20], we consider the structural paragenesis as a pattern consisting of structural elements defined by a common dynamic factor. The structural pattern could be formed by single or several parageneses. It should be remembered that the conjugate shears often used in the analysis are formed under the impact of compression or extension as a system of intersecting subsynchronous [36] fractures [33, 40]. The intersection of shears results in the formation of two pairs of alternate dihedral angles. The maximum strain σ_1 is directed along the bisectorial plane of the pair of alternate angles orthogonally to the shear conjugation (intersection) line. The angle

between the main compression axis and one of the two conjugate shears is termed as the shear or shearing angle θ, while 2θ is the conjugation angle. Under conditions of brittle deformations, θ is no more than 45°. However, under the ductile shearing typical, for instance, of middle crustal conditions (mesozone [27]), the angle θ may reach 70−80° [33]. The minimum compression σ_3 is directed along the bisectorial plane of the other pair of alternate angles. The medium compression axis σ_2 is parallel to the conjugation line. The conjugation angle, the orientation of the shears, and their updip−thrust kinematic parameters are used to determine the directions of the main normal compression axes: σ_1, σ_2, and σ_3. The symbols of the axes are supplemented by the geochronological index.

The parageneses and patterns were studied by field measurements, graphical, and statistical methods. The graphical method consists in the compiling and analyzing of maps, plans, and sections. The statistical method reconstructs the model parageneses on the stereographic projections [30] and is discussed in detail in [37]. Our statistical models are represented by diagrams superposed on the Wulff stereonet (upper hemisphere) using numerous measurements of the structural elements.

## RESULTS OF THE STUDY: THE GEODYNAMIC PERIODS AND STRUCTURING DYNAMICS

The reference characteristics of the structure and structure-forming stress fields are described by us in

Fig. 1. Structural dynamic schematic map of the southern framing of the Khanka Massif. Compiled by P.L. Nevolin using materials of G.S. Belyansky et al. (2006), T.K. Kutub-Zade et al. (2002, 2010), [15] and the author's observations (a).

(*1−3*) blocks (remnants) of the Riphean−Cambrian crystalline rocks: (*1*) granite gneiss, (*2*) metapelite and gabbro gneiss, (*3*) gabbro-, diorite-, and granite gneiss; (*4*) Riphean−Cambrian Sergeevsky gabbroid; (*5−9*) Paleozoic stratified complexes: (*5*) Cambrian carbonate−terrigenous, (*6*) Silurian siliceous−volcanogenic−terrigenous, (*7*) Devonian volcanogenic basic−intermediate, volcanogenic−carbonate−terrigenous, (*8*) Carboniferous, mainly volcanogenic rocks of felsic composition, tuff, and tuffconglomerate, (*9*) Permian carbonate−terrigenous and volcanogenic intermediate−felsic; (*10−15*) Mesozoic stratified complexes: (*10*) Triassic silt-sandstone, including coaliferous ones; (*11*) Triassic volcanogenic acid−intermediate; (*12*) Jurassic sandstone−siltstone; (*13*) Early Cretaceous coaliferous siltstone−sandstone; (*14*) Early−Late Cretaceous volcanogenic−sedimentary; (*15*) Late Cretaceous volcanogenic felsic; (*16−18*) Cenozoic deposits: (*16*) Tertiary coaliferous sedimentary; (*17*) flood basalts; (*18*) Quaternary sediments; (*19−22*) intrusive rocks: (*19*) Vendian−Ordovician biotite−hornblende granite; (*20*) Permian hornblende granodiorite-granite, (*21*) Permian (?) gabbro and gabbrodiorite, (*22*) undivided Mesozoic granites; (*23*) Triassic kinematic complex; (*24*) axes of antiform arches (a) [(Lsh) Lishuchzhen, (Kch) Kachalinsk , (Sp) Spassk] and synform troughs (b) [(Pg) Pogranichny, (Vz) Voznesenka], which were formed due to Paleozoic latitudinal compression; (*25*) direction of compression of geodynamic periods: (PR) Proterozoic−Early Paleozoic, (PZ) Middle−Late Paleozoic, (MZ) Mesozoic−Cenozoic; (*26−27*) faults (dash lines—inferred, including faults beneath Cenozoic deposits): (*26*) sinistral stike-slips: (WP) Western Primorye, (KCh) Kachalinsk, (US) Ussuri, (KB) Kubansky, (*27*) thrusts; (*28*) general orientation of overturned limbs of the Kachalinsky arch; (*29*) axes of folded and pseudofolded forms in the pre-Mesozoic complexes; (*30*) axes of the Mesozoic arches (a) and troughs (b) of folds; (*31*) boundaries of the Triassic complexes localized in the discordant arches and troughs; (*32*) state boundary of Russia with China and Korea; (*33*) coastal strip; (*34−35*) rough outlines of the discussed basins: (*34*) Early Cretaceous: (RZ) Razdol'noe, (*35*) Cenozoic: (TR) Turiy Rog, (ZR) Zharikovo, (PV) Pavlovka, (RZ) Razdol'noe; (*36*) inferred outlines of arches and troughs in plan.

Terranes joining and overlying the complexes of southern Primorye (after [34, 35]) (b).

(*1−6*) overlying complexes: (*1*) Cenozoic, (*2*) Mesozoic volcanic, (*3*) Late Albian−Paleocene subduction, (*4*) Late Albian−Paleogene accretionary wedges, (*5*) Jurassic turbidite basins, (*6*) Late Permian subduction, (*7−8*) collisional granites: (*7*) Mesozoic−Cenozoic, (*8*) pre-Devonian; (*9−13*) terranes: (*9*) Cambrian−Early Ordovician continental margin volcanic and plutonic arcs, (*10*) Early Silurian island arcs, (*11*) Precambrian active continental margins, (*12*) Early Cretaceous turbidite basins, (*13*) blocks of the crystalline basement, (*14*) inferred boundaries of the terranes beneath overlying complexes; (*15*) terrane abbreviations: (MN) Matveevka−Nakhimovka, (LH) Laoelin−Grodekovo, (VS) Voznesenka, (SP) Spassk, (SR) Sergeevska, (SM) Samarka; (*16*) age of the overlying complexes: JTr—Triassic−Jurassic, eK—Early−Late Cretaceous, (Cz) Cenozoic.
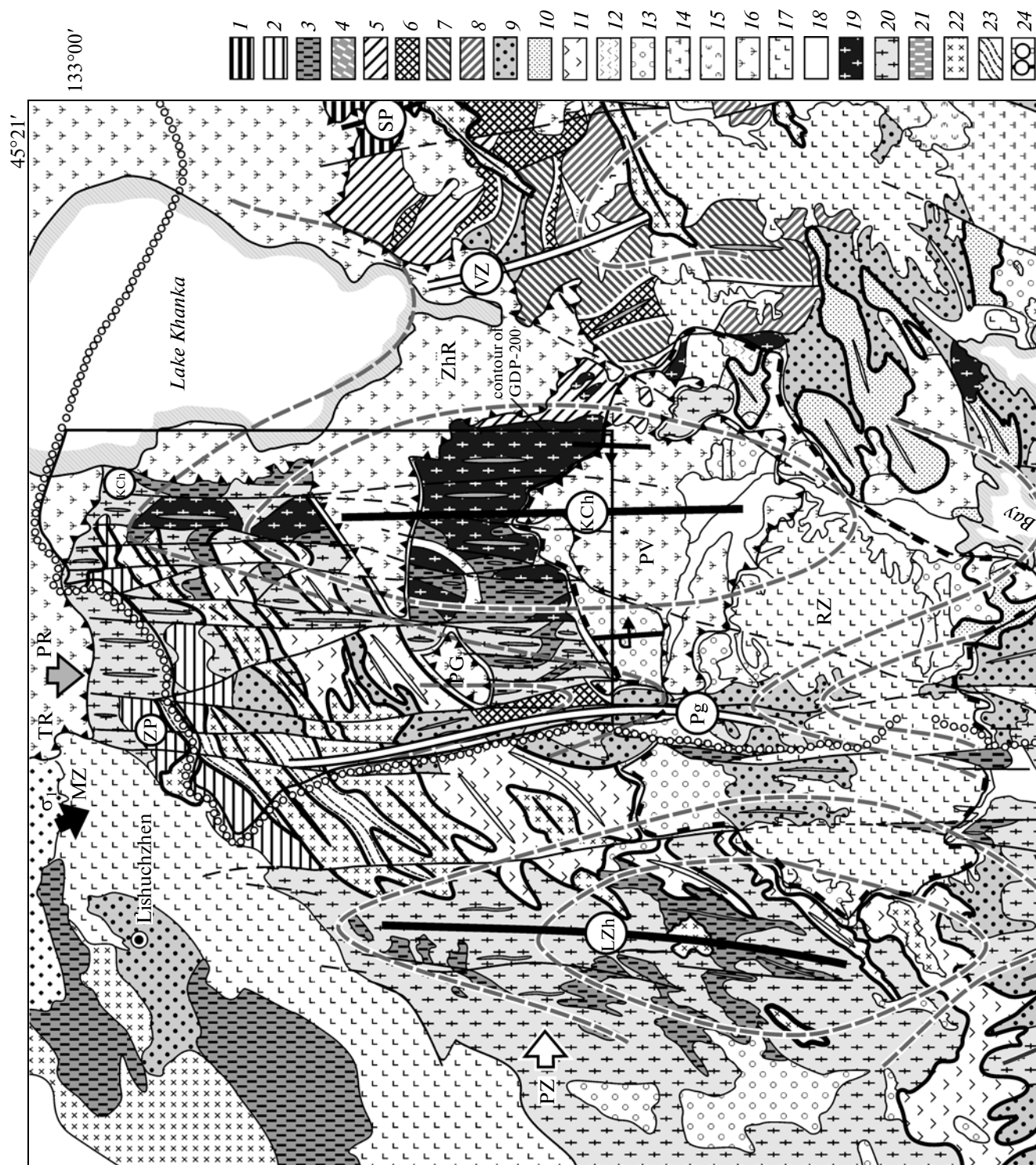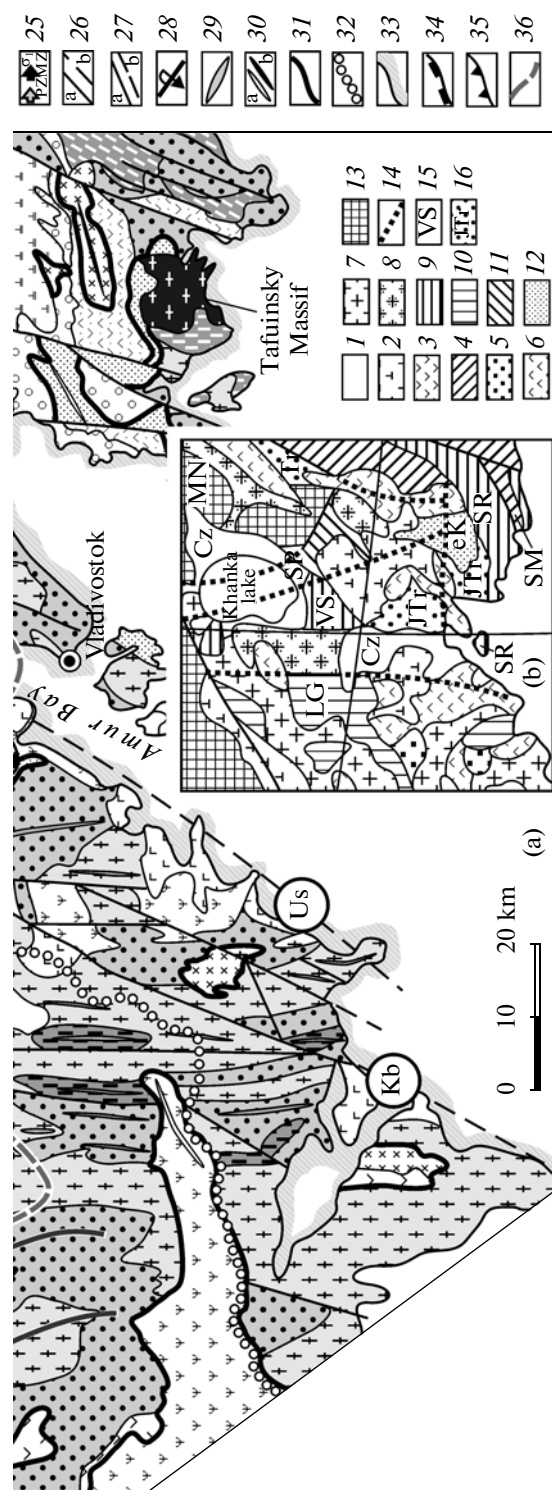
Fig. 1. Contd.

the order of their evolution. The structure of the area is formed by three subsequent structural patterns (Figs. 1, 2), each of which is determined by an independent stress field [23, 29]. The geochronological range of the formation of each pattern is termed as the **geodynamic period**. We distinguished the Proterozoic–Early Paleozoic, Middle–Late Paleozoic, and Mesozoic–Cenozoic periods. With a variable degree of confidence, each period is subdivided into 2–3 *activation episodes*, which in turn consist of time *intervals* comprising higher-order *pulses*.

The Proterozoic–Early Paleozoic geodynamic period is characterized by the meridional orientation of the maximum compression axis σ_1^{Pr}. The period is divided into two dynamic episodes of compression activation.

The first episode of compression activation marks the structuring of the metamorphic basement. The structural parageneses formed during the first period were preserved in the large and small remnants of the Riphean–Cambrian rocks (Figs. 1, 2). The largest (up to a few tens of km²) metamorphic massifs were mapped in the northwestern part of the area (blocks I and II in Fig. 2). The first (I) massif is made up of Cambrian metapelites, while the second massif (II) comprises Riphean banded gabbro-granite gneisses. The style of the structural pattern of both the blocks is shown in the diagrams of the foliation orientation (Figs. 3a, 3b), where the isolines around the main maximums (I and V) form extended bands confined to the equators of the main belts (1). The arrangement of the belts indicates the folded type of distribution of the foliation belts among the predominant structural patterns. The asymmetry of the folds marked by the predominant concentration of poles in one of the maximums (I) indicates the northern vergence of the plicative structures. This pattern is similar to that of the orientation of similar elements located in Primorye's largest exposures of the Khanka basement: the windows of the Matveevka–Nakhimovka terrane (Figs. 1b, 3c). The style of the parageneses of small folds shown in the diagrams is confirmed by their direct observations in the bedrocks in all three abovementioned blocks. It is noteworthy that the same orientations and style of folded parageneses were observed in the small granite-framed remnants (tens and hundreds of m²) of ancient gabbro–granite gneiss, diorite–granite gneisses, metapelite, and marbled limestones (Fig. 4). It follows that the orientation and configuration of the structural patterns even in the small blocks–remnants did not experienced significant changes during the subsequent dislocations. Their dislocation pattern unambiguously corresponds to the most typical structural pattern of the Khanka Massif. Therefore, the deciphering of the stress fields of the pre-Middle Paleozoic geodynamic period using the structural patterns of the remnants seems to be correct. It indicates the prevailing submeridional compression σ_1^{Pr} during this period. Based on many of the below discussed features, the medium strain axis (σ_2^{Pr}) gently dips in the NNE direction, being best expressed by the position of the belt axes (1) in the dia-
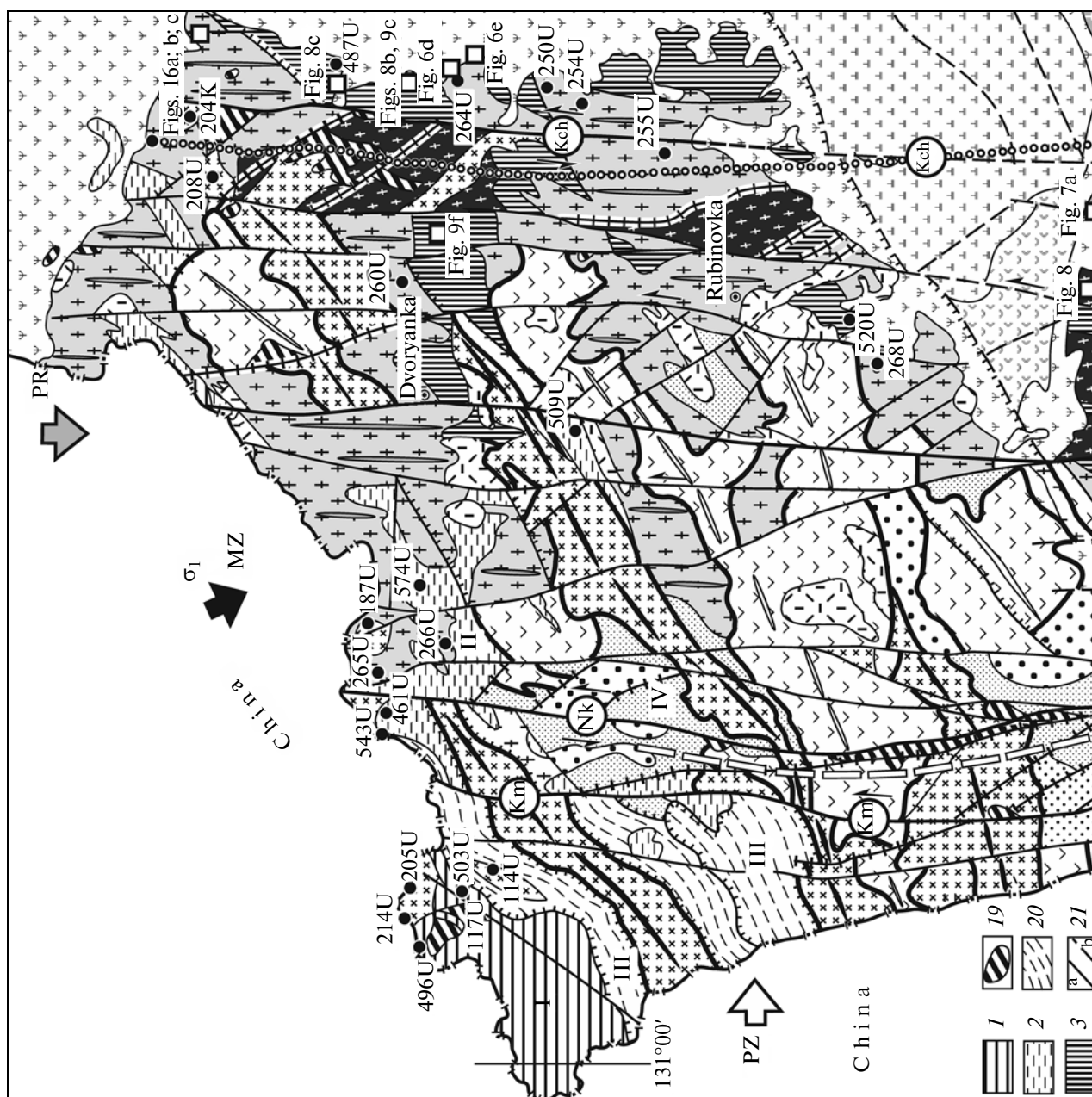
Fig. 2. Structural–dynamic schematic map of the near-Khanka fragment of the boundary band of the Western Primorye area. Compiled by P.L. Nevolin using materials of T.K. Kutub-Zade et al. (2006, 2010) and the author's observations.

(*1–3*) blocks–remnants of the Riphean–Cambrian metamorphic rocks: (*1*) metapelite, (*2*) granite-gabbro-gneiss, (*3*) metapelite and gabbro-granite gneiss transformed during the Paleozoic geodynamic period; (*4*) Silurian siliceous–volcanogenic–terrigenous rocks: (*5*) Lower–Middle Permian terrigenous sediments; (*6*) Middle Permian volcanogenic and volcanogenic-sedimentary rocks: (*7–8*) Triassic intermediate volcanics: (*7*) stratified, (*8*) extrusive; (*9–10*) Lower Cretaceous coal-bearing deposits: (*9*) mainly sandy, (*10*) mainly silty; (*11–14*) Tertiary carbonaceous sediments: (*11*) Paleogene, (*12*) lower Neogene, (*13*) middle Neogene, (*14*) Upper Neogene; (*15–19*) intrusive rocks: (*15*) Vendian (?) gneiss-granite with remnants of marbled limestone, (*16*) Ordovician biotite–hornblende gneiss granite, (*17*) Permian hornblende gneissose granodiorite-granite, (*18*) undivided Mesozoic granite, (*19*) Cretaceous granite porphyry, (*20*) Triassic kinematic complex: mica schists; (*21–24*) faults (a dash denotes inferred faults, including those beneath unconsolidated sediments): (*21*) with uncertain direction of displacement, (*22*) thrusts and reverse faults, (*23*) extension fractures, normal fault, (*24*) strike slips. A solid line denotes large strike slips: (KM) Kamenushkinsky, (Nk) Nikolaev (both dislocations border the regional Western Primorye fault zone), (Bg) Boguslavka, (Kch) Kachalinsk; (*25*) axes of folded and pseudofolded forms in the Mesozoic complexes, (*26*) axes of Mesozoic antiform (a) and synform (b) folds: (*27*) boundaries of intrusive and stratified Triassic complexes localized in the discordant arches and troughs; (*28*) Russia–China state boundary; (*29*) points of photos and their numbers in the text; (*30*) absolute age determinations: U—uranium, K—potassium–argon; (*31*) axes of the Kachalinsk antiform arch (Kch) (a) and Pogranichny synform trough (Pg) (b), which are derivatives of Paleozoic latitudinal compression, (*32*) direction of compression during geodynamic periods: (PR) Proterozoic–Middle Paleozoic, (PZ) Middle–Late Paleozoic, (MZ) Mesozoic–Cenozoic; (*33*) points of figures in the text, according to the numbers; (*34*) numbers of blocks of ancient rocks for which stereonets were plotted (Fig. 3).

Fig. 2. Contd.

grams (Figs. 3a, 3b). Correspondingly, the axis of the minimum stress σ_3^{Pr} is oriented vertically.

The second episode of the compression activation of the Late Proterozoic−Early Paleozoic geodynamic period was determined by the beginning of the disintegration of the crystalline basement with the initiation of riftogenic basins. The basins, which were the precursors of the Pogranichny, Voznesenka, and other troughs, are determined by extension zones (Figs. 1a, 2). The intervening uplifted blocks have a submeridional orientation parallel to the axis of the main normal

compression and the plane $\sigma_1\sigma_2$, which is logical for the Late Proterozoic−Early Paleozoic regional stress field. The uplifted blocks between the basins have the same orientation. The basins are filled with stratified sequences. Note that the Voznesenka basin is represented by siliceous−carbonate−volcanogenic−terrigenous complexes of almost the entire Paleozoic, except for the Ordovician (Fig. 1), while the Pogranichny basin accumulated only Silurian and Permian stratified rocks (Figs. 2, 5), and the gap between deposits of different ages is weakly expressed in the structure and stratigraphy. The differences are possibly
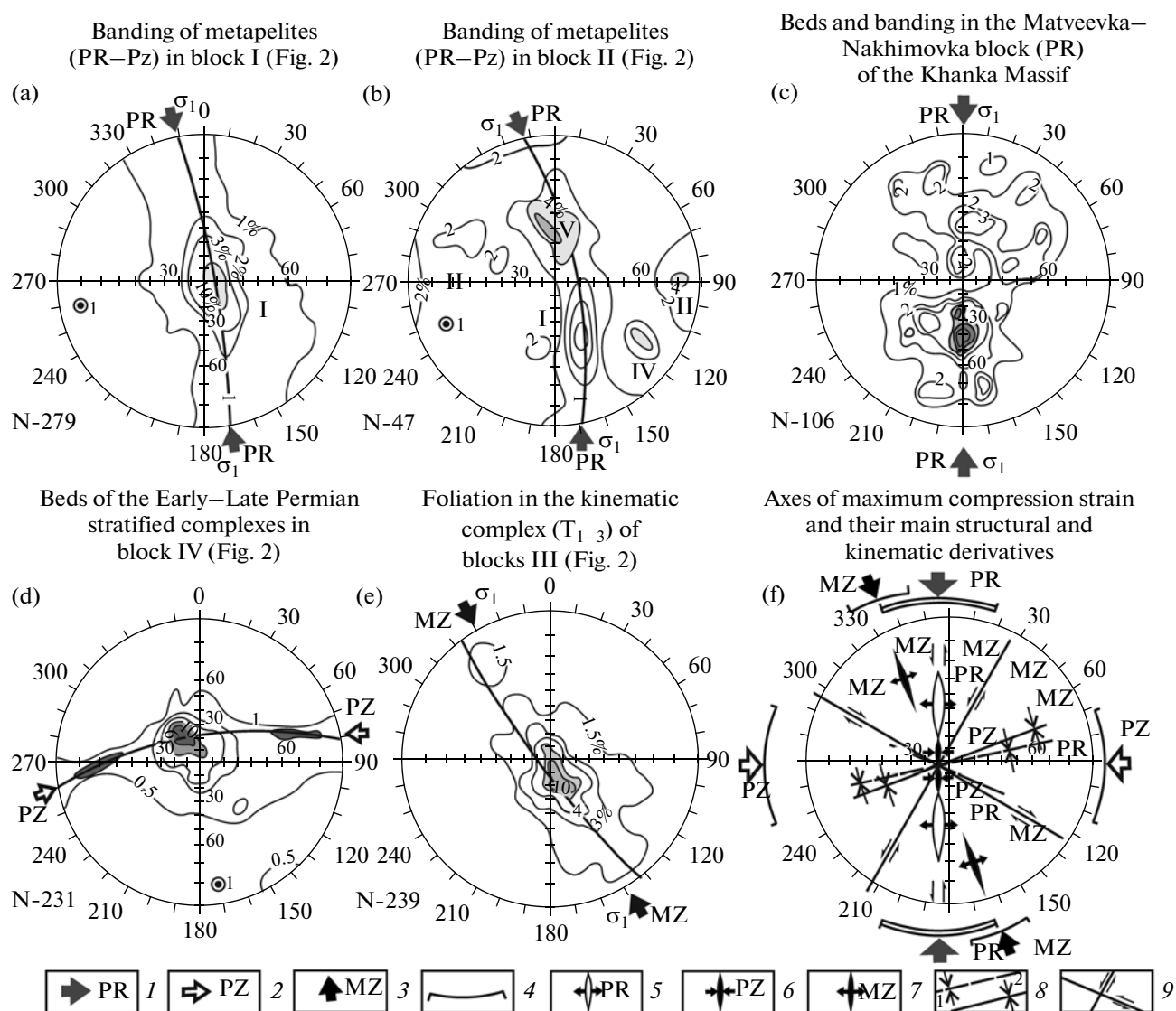
Fig. 3. Diagram illustrating the orientation of the structural and geodynamic elements (Wulff stereonet, upper hemisphere). (*1−3*) maximum compression during the geodynamic periods: (*1*) Late Proterozoic−Early Paleozoic, (*2*) Middle−Late Paleozoic, (*3*) Mesozoic−Cenozoic; (*4*) sector of possible variations of the compression orientation; (*5−9*) orientation of structures of different dynamic loadings considered in the text: (*5*) Late Proteorozic−Early Paleozoic extension structures, (*6*) Middle−Late Paleozoic compression structures, (*7*) Mesozoic−Cenozoic extension structure, (*8*) Early Paleozoic (1) and Mesozoic (2) compression structures, (*9*) Mesozoic structures of tangential strike-slip impact (see the text for the explanation).

related to the numerous thrusts of western vergence spanning the Pogranichny structure. Owing to the disintegration, the extended basement crossed by normal faults acquired a mosaic structure, which is indirectly supported by the high-gradient wedgelike gravity anomalies bounded by linear salients [18].

The parageneses of the fault framework, which played significant role in the disintegration of the crystalline basement, were mainly defined during the second episode. In particular, the formation of the above mentioned riftogenic basins should be accompanied by the development of extended longitudinal normal faults. This process can provoke the formation of a dynamic pair of NE-trending sinistral and NW-trending dextral strike slips. Later, the fractures of the indicated types were repeatedly rejuvenated and transformed.

Middle−Late Paleozoic geodynamic period. The structural pattern of the period is well expressed in Western Primorye. The main structure-forming factor of this period was *sublatitudinal compression*, σ_1^{PZ}, and the flattening deformations initiated by them. Under conditions of flattening, which was expressed in warping, folding, and formation of cleavage and gneissosity, the pre-Middle Paleozoic *rift depressions* and intervening uplifted blocks of ancient rocks oriented nor-
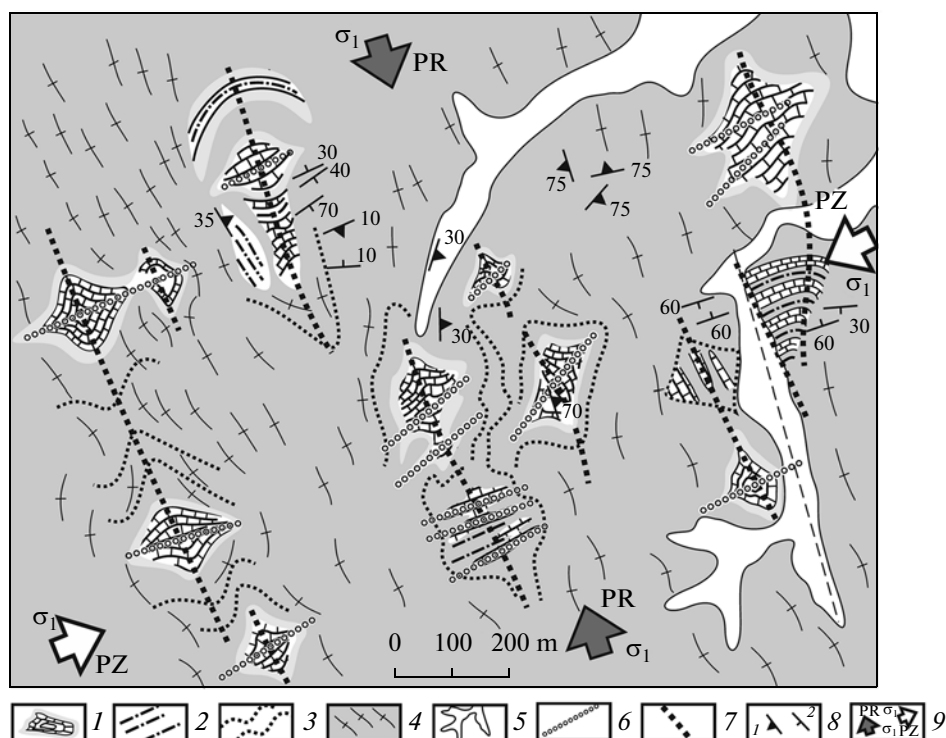
Fig. 4. Remnants of marbled Riphean (?) limestones among Vendian (?) gneissic granites. The scheme was compiled using the materials of M.D. Ryazantseva (1970).

(*1*) remnants of marbled limestones, their shadow contours, and orientation of the bedding; (*2*) mylonitization in limestones; (*3*) inferred trajectory of shadow structures: mylonitization in limestones and gneissosity in granites and their orientation; (*4*) gneiss granite; (*5*) Quaternary sediments; (*6–7*) inferred axes of folded forms derived by lateral compression: (*6*) submeridional compression σ_1^{PR}, (*7*) sublatitudinal compression σ_1^{PZ}; (*8*) orientation of gneissosity (1), bedding (2); (*9*) direction of the compression of the Proterozoic−Early Paleozoic (1) and Middle−Late Paleozoic (2) periods.

mally to the maximum *sublatitudinal* compression σ_1^{PZ} acquired contrasting morphology of arches and troughs. The Kachalinsky arch and Pogranichny trough (Fig. 2), as well as the Lizhuchzhen and Spassk arches and the Voznesenka troughs in their framing, were distinguished in the studied area. The negative morphological structures accumulated and deformed sedimentary rocks, while the arches served for magma penetration. The morphological structures of the first order were complicated by parageneses of the 2nd to 5th orders.

Based on the geochronological dating of granites, the considered geodynamic period is subdivided into two episodes of activation: the Ordovician and Silurian−Permian. Structurally, these episodes practi-

Fig. 5. Tectonic structures of the Sof'ye−Alekseevka area and dynamics of their formation. Compiled by P.L. Nevolin using the materials of A.T. Kandaurov et al. (1984).

(*1*) Cenozoic sediments; (*2*) Triassic rhyolite, dacite, andesite, trachyrhyolite, and tuffs of all these varieties; (*3*) Middle Permian rhyolite and andesite tuffs, sandstone, and siltstone of the Barabash Formation; (*4*) Lower and Middle Permian coaly siltstone and sandstone of the Reshetnikovka Formation; (*5*) Lower Permian rhyolite, rhyolite tuff, and sandstones of the Kazachkinskaya Formation; (*6*) Lower Silurian mainly sandstone, gravelstone, and basalt of the Upper Kordonka subformation; (*7*) Lower Silurian coaly siltstone, siliceous−clayey shales, basalt, and tuffs of andesite, lenses of cherts of the Lower and Middle Kordonka Subformation; (*8*) lenses of cherts (1) and conglomerates (2); (*9*) Late Permian gabbro; (*10*) Late Permian medium-grained granite of the Ryazanovka Complex with enclaves of the protorocks of the gabbroid basement (?); (*11*) strike-slip (1), thrust (2) and reverse fault (2); (*12*) fault of unclear kinematics; (*13*) areas of sections with the prevailing unipolar dip of the beds (the numbers denote the dip angle); (*14–15*) axes of antiform (1) and synform (2) folds (the numbers denote the dip angles of the limbs): (*14*) small, (*15*) large; (*16*) orientation of the beds: overturned (1) with uncertain and normal attitudes of the bottom and roof (2); (*17*) finds of fossil fauna; (*18*) ore bodies: established (1), inferred (2); (*19*) axes of inferred shadow antiform folds in granites; (*20–21*) direction of regional compression: (*20*) Late Paleozoic, (*21*) Mesozoic; (*22*) complicated by fine folding in the area of closure of large folds; (*23*) main water streams.

Diagrams of the orientation of the structural elements (Wulff stereonet, upper hemisphere): (a) bedding and foliation in the rocks of the Kordonka Formation (345 measurements), (b) bedding and foliation in the rocks of the Kazachkinskaya Formation (207 measurements); (c) fractures and dikes (box), 307 measurements
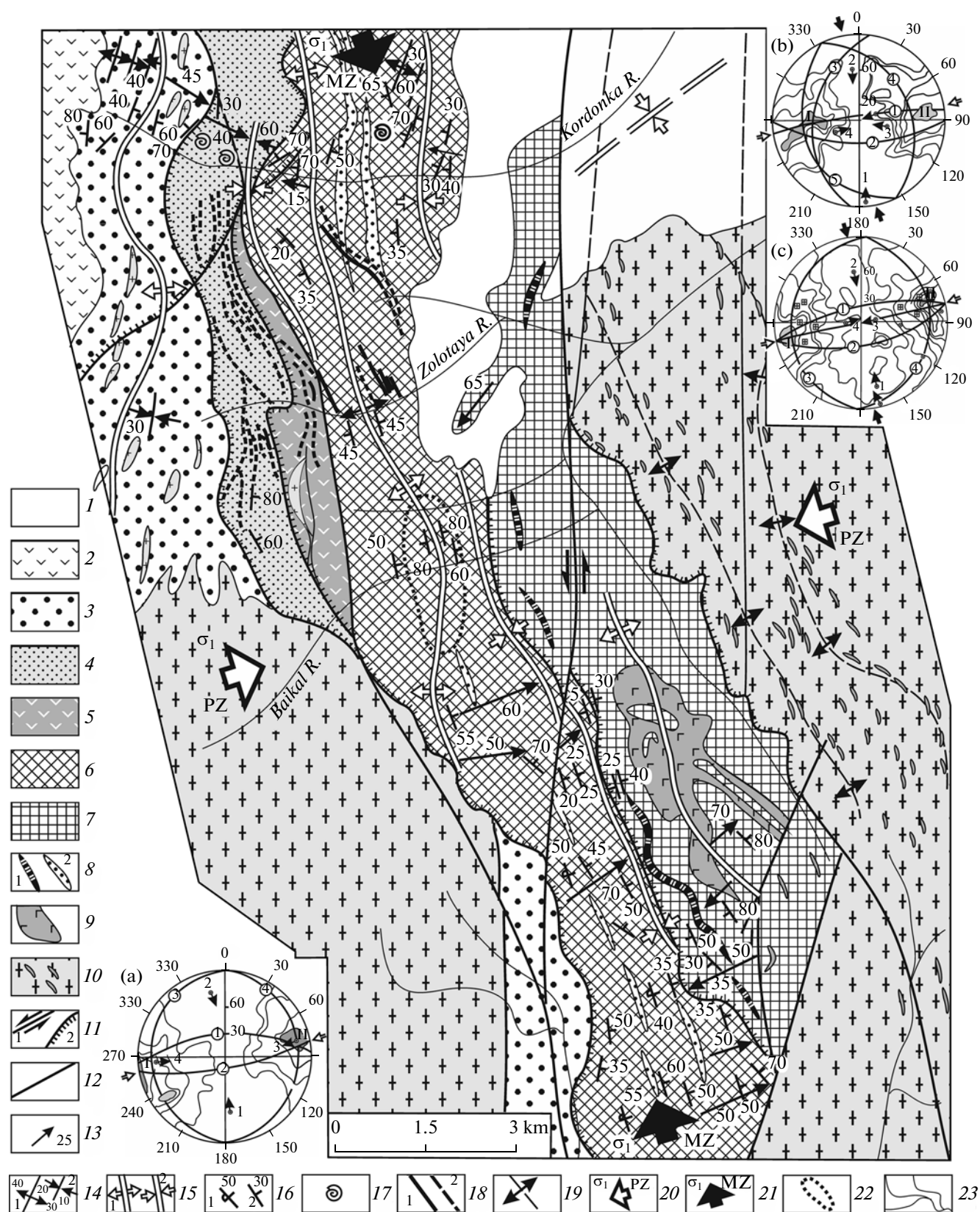
cally are not expressed. *The first and second episodes* were mainly controlled by flattening and formed the entire main Paleozoic arch–trough structure of the region, while *the second episode* additionally produced medium and small structural parageneses, whose features are reflected immediately in the structure of individual troughs and arches.

The Pogranichny trough accumulated Silurian and Early and Late Permian volcanogenic–sedimentary rocks. In general, this trough has an asymmetrical NW-vergent morphology complicated by higher order folds, which are accompanied by synfolded overthrusts and upthrusts. The latters include the Kamenushkinsky and Nikolaev faults, which compose the Western Primorye fault zone.

The higher order folded forms that compose the Pogranichny trough are from a few hundreds of meters to one kilometer in size and define the style of the structural pattern of the trough (Figs. 2, 5). One of them, the second-order Kordonka anticline, occupies the middle part of the Pogranichny trough (Fig. 5). The core of the fold is made up of the Silurian rocks, while the limbs, Permian rocks. The western overturned limb of the fold is represented by the most complete series of Permian stratified rocks, while the eastern limb of normal attitude is characterized by the incomplete rock sequence due to the strong thrusting deformation. The limbs of the Kordonka anticline are associated with the folded parageneses of the third, fourth, and fifth orders, which presumably were produced during the second episode of activation. The folds of the third (up to 100 m wide), fourth (up to 10 m), and fifth (up to 0−3 m) orders are conformable to each other, which is reflected in their constant height to width ratio of ~ 1.5 : 1. Correspondingly, the limbs are moderately and strongly steep. The complicating folds are mainly represented by linear submeridional asymmetrical often westward overturned folds with gentle hinges; isoclinal folds also occur. In the Early Silurian Kordonka Formation (Fig. 5a) and Permian rocks, limbs dip eastward in contrast to the opposite stratigraphic build-up, which is caused by the predominant thrusting along low-angle and moderate-angle submeridional faults. Correspondingly, the axial surfaces of the subordinate folds dip mainly to the east and, more rarely, to the west and vertically. The slickensides of smaller folds are consistent with the orientation of the limbs of larger folds, while the styles of the small folds are consistent with and controlled by the predominant thrust−reverse fault subinterlayer movements on the limbs. Fold slickensides often coincide with small thrust faults. This follows from the coincidence of the main maximums in the diagram (Figs. 5a, 5c). Judging from the symmetrical distribution of the bedding poles in the diagram, the beds of the Kazachkinskaya Formation are deformed into isoclinal folds, (Fig. 5b). The folds are often associated with axial surface cleavage, which was foliated and plicated. The foliation surface is often mylonitized and covered by chlorite−hydromica−sericite crusts.

The Voznesenka trough is structurally similar to the Pogranichny trough. It has the same longitudinal strike and, in addition, contains longitudinally oriented stratified Paleozoic complexes. The structure of the latters was not studied in detail, but the analysis of the bedding orientation shows that, dissimilar to the Pogranichny trough, this trough has a symmetrical structure of almost regular syncline.

The Kachalinsk arch is located between the Pogranichny and Voznesenka troughs. It is traced in the N−S direction by metamorphosed Silurian complexes located among granites. Apart from the domination of clear flattening, it would be identified as a granite gneiss dome from its ellipsoid shape. However, all the parageneses indicate a rather lateral and not vertical type of maximum compression, because the maximum compression during dome formation should be vertical. The intruding plutonic body had no structure-forming force but only replaced and granitized pre-Silurian rocks thinned in the arches.

The granitization in the Kachalinsk arch led to the formation of the Silurian Grodekovo batholith, which has a horseshoe morphology terminating toward the inferred northward subsidence of the Kachalinsk arch (Fig. 2).

The boundaries between the granites of different ages are vague. The Ordovician and Late Permian granite complexes were distinguished on the basis of U−Pb zircon dating. Some granite areas are characterized by extremely high degrees of gneissosity, which points to their possible Vendian age (Fig. 2). It is noteworthy that the granites demonstrate *primary* and *secondary* fold parageneses.

The *primary parageneses* appear as shadow patterns that are better observable on the weathered surface of exposures. "Shadows" presumably represent the remnants of structural forms of precursors during the granitization (Figs. 6a, 6b). In the fresh chips, they are supported by dashed foliation accentuated by trajectories conformable to extended mafic minerals. The shadow folds are multiorder folds. Even one exposure may contain up to 5 or more complicating orders to the microscopic level (Fig. 6b). These smallest folds manifested in the yellowish gray metapelite bed (?) are remarkably convergent to large forms. In the cores of the shadow folds, the protorocks are often least altered and form N−S extended low-angle cigar-like bodies in the granites, thus representing low-angle medium strain and deformation axes (σ_2^{PZ}). The protorocks that compose such cores have a sufficiently variegated appearance of deformed metamorphic rocks (Figs. 6a, 6b). The limbs of the shadow folds sometimes reveal shadow macrobanding in the granites, the "beds" of which are often interpreted as granitized flysch unit rhythms.
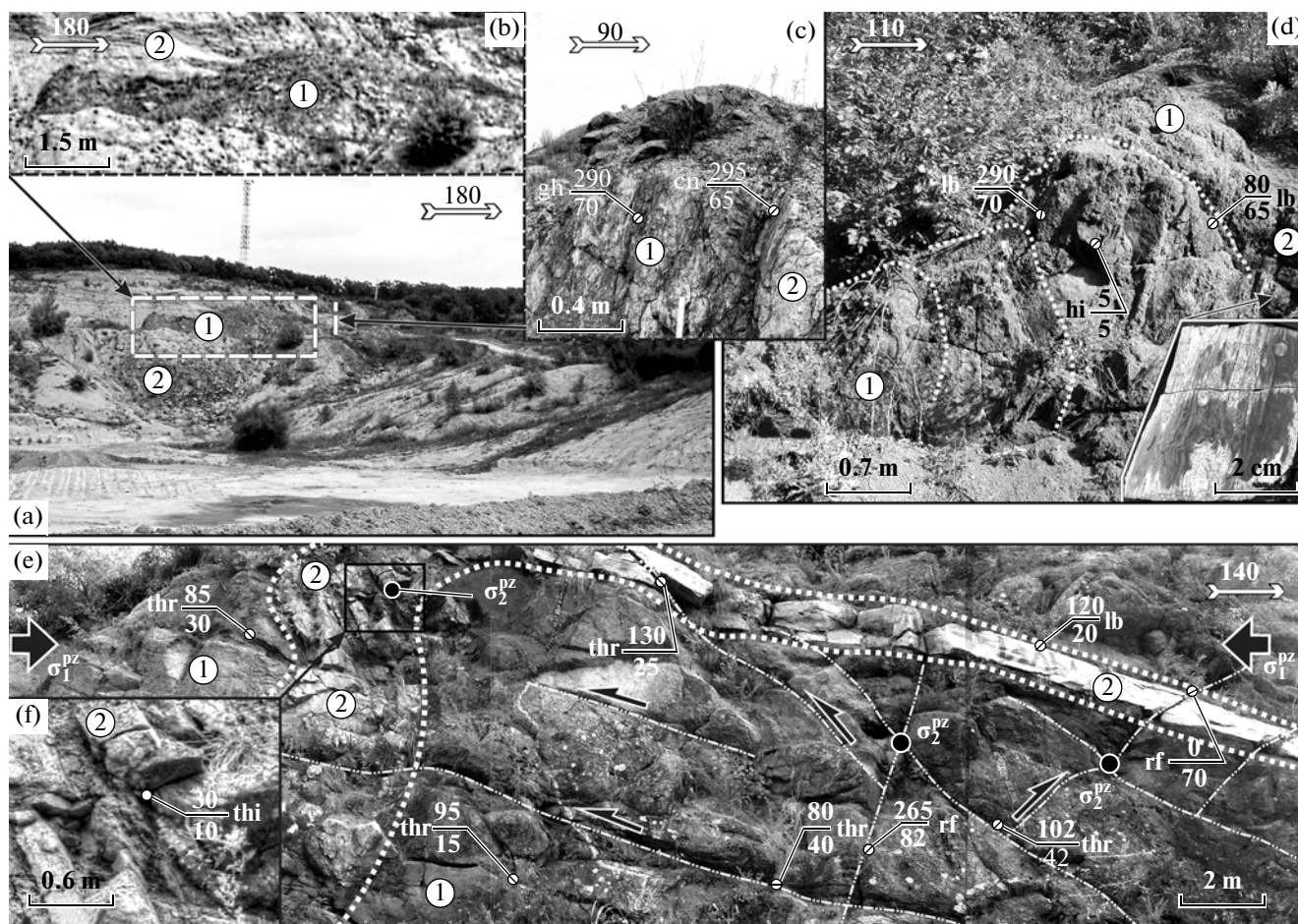
Fig. 6. Shadow folds and pseudofolds in the Late Permian hornblende granites (P$_3$) of the Ryazanovka Complex.

(a, b) N−S extended remnant of ancient metamorphic rocks (1) among granites (2) forming the core of a small tightly compressed fold, (c) structure of the remnant across the strike: strongly sheared and cleavaged microgabbro (1), boudins of gneissose fine-grained granites (2); (d) shadow folded forms in the granites (1) expressed only on the weathered surface, as well as layerlike aplitic segregation in granites, which has a concordant microfolded structure (fragment). (e) pseudofolded morphology of the layerlike aplite body (2) in the granites. Hinge of pseudofolds in fragment F. Systems of conjugate shears (dash) with thrust−reverse fault kinematics (arrows) are distinctly seen in the photo. The medium deformation axis expressed by the similarly oriented hinge of pseudofolds and conjugation lines between shear−thrusts is gentle and meridional.

Hereinafter, the symbols shown in the photo illustrations are as follows: the wide arrows show the direction of the axis of the maximum compression; the black points show the outcrops of the conjugation lines indicating the position of the medium deformation axis σ_2^{PZ}; the acute arrows show the direction of the displacement along the shear; the white points show the points of the measurement of the orientation of the structural elements; the numbers in the numerators denote the azimuth, while the numbers in the denominator, the dip angle of the plain element; the indices: **gn** gneissosity, **hi** fold hinge, **thr** thrust, **rf** reverse fault, **cn** contact, **lb** fold limb, **cl** cleavage, and **fol** foliation; the circled dash denotes the position of the structural element in the image plane.

Secondary pseudofolds were formed later. Their main difference from the primary folds consists in their initiation along systems of closely spaced counter-dipping thrusts. Therefore, the limbs of the pseudofolds are either planar or expressed by surfaces in the form of broken lines. Some pseudofolds marked by vein quartz−feldspar material overprinted primary forms without distortion of their configuration. Examples of such folds of different scales are shown in Figs. 6f, 7a, 7b, and 8. In Fig. 6f, the shear pseudofold is designated by aplites in the Permian granites. It is formed by two conjugate shear systems. The eastern limb of the fold is low-angle planar, while the western limb has a steep dip expressed by the curved broken line. The conjugation of the limbs is smoothed and appears as hinges. This pseudofold is operprinted discretely by two systems of conjugate shears that were formed by stress fields with close orientation of the axes. The superimposed shears cause a systematic reverse-fault displacement of the aplites in the eastern limb of the fold. The conjugation angle of each superimposed shear system is more than 90°, which indicates the mechanism of ductile shearing. In other words, the earlier "folded" shear paragenesis and
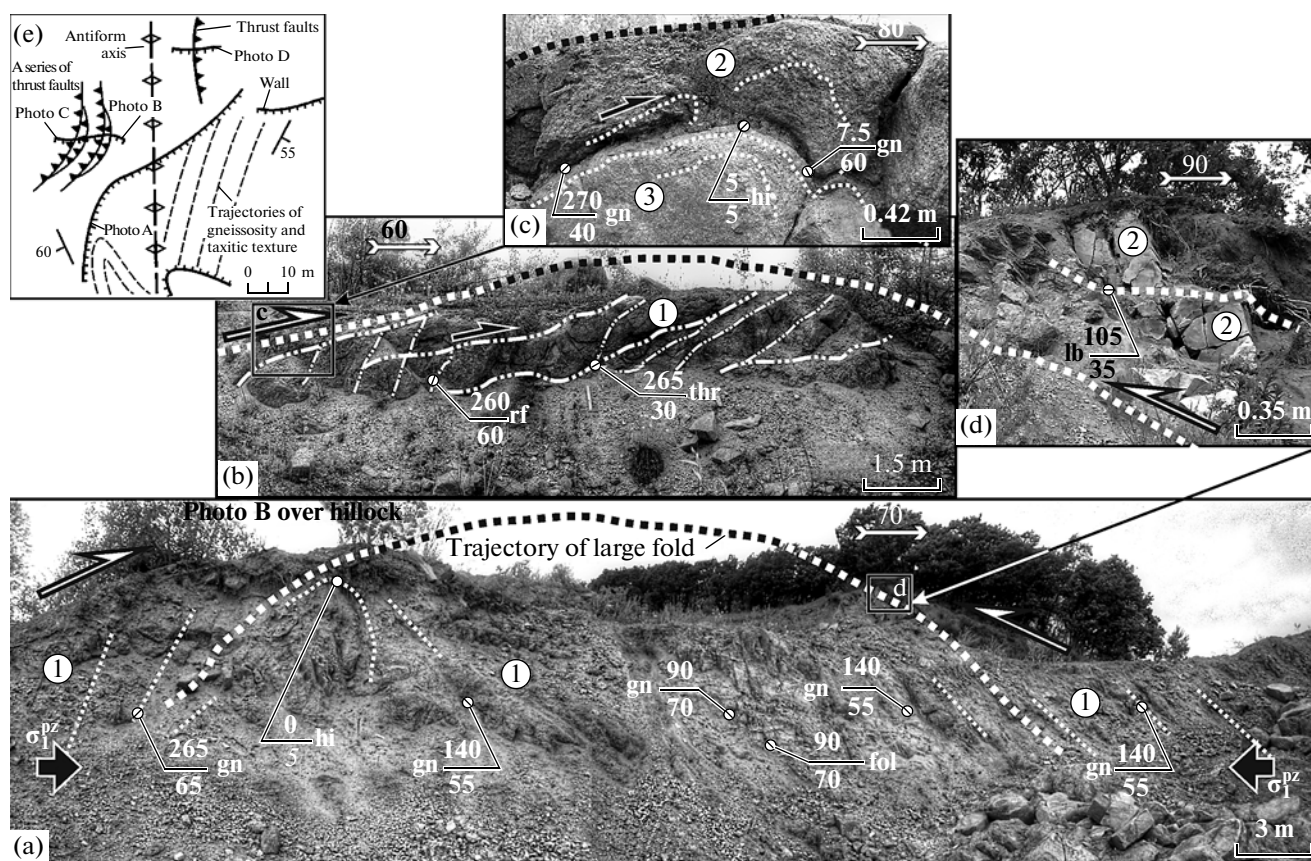
Fig. 7. Antiform fold−thrust structure of the third and fourth orders in Ordovician granite gneisses under conditions of latitudinal lateral compression and granitization of the ancient rocks. Collage of photos of the quarry walls in the right side of the Nesterovka River (see Fig. 2).

(a) general view of the antiform as deciphered from the trajectory of the taxitic texture, foliation, and gneissosity in the granite gneiss (the dash in image a). The granitization was presumably developed after fyschoid, which is supported by fragments of locally desiphered primary grading and the normal position of the protorhythms. (b) beyond direct visibility. Figure b and inset c show the thrust zone of the left limb of the antiform, in which the taxitic texture and gneissosity in the granites are concordant with the direction of the prevailing thrust planes. (d) fragment of the thrust of the right limb; the displacement along it is directed toward the thrust in Fig. b, which is recorded by the displacement of the aplite "layer." (1) coarse-grained granite gneiss, (2) aplite, (3) fine-grained granite gneiss. The arrows show the compression direction; (e) the plan of the location of the photos. The other symbols are shown in Fig. 6.

superimposed shear parageneses were formed in a ductile medium. A significant point consists in the similar sublongitudinal orientation of the medium deformation axis σ_2^{PZ}, which is expressed by at least three different features: fold hinges and the intersection lines of two systems of superimposed conjugate shears. This indicates the discrete pulsed impact of the compressional strains. In other cases, small possibly shear folds marked by aplites also complicate the structure of the Cambrian metasedimentary rocks (Fig. 8a). The shapes of the small folds are geometrically and dynamically similar to those of large folds, one of which is illustrated by a collage of photos of a quarry excavated in the Ordovician granite gneisses (Fig. 7). In the photos of the wall and plan of the quarry, the trajectory of the gneissosity and taxicity texture show the vergence of the folds, which compli-

cate the arch of the larger antiform. Counter movements along thrusts accompanying limbs are unambiguously defined.

In other words, the granites demonstrate typical fold−thrust paragenesis, which is fragmentarily but well consistent with the folded shape of the longitudinal compression. These structures were presumably formed almost simultaneously with the granitization, though some folds were likely shadow, which follows from the bent granitic "beds."

The gneissosity and cleavage accentuating the dynamics of the latitudinal compression are widely distributed. They are not indicators of the granite's age but depend mainly on the character, primarily the intensity of the stress fields. The gneissosity is expressed by the linearized aggregates of quartz, feldspars, plagioclase, and mafic minerals. The degree of linear ordering of these minerals is different. It should
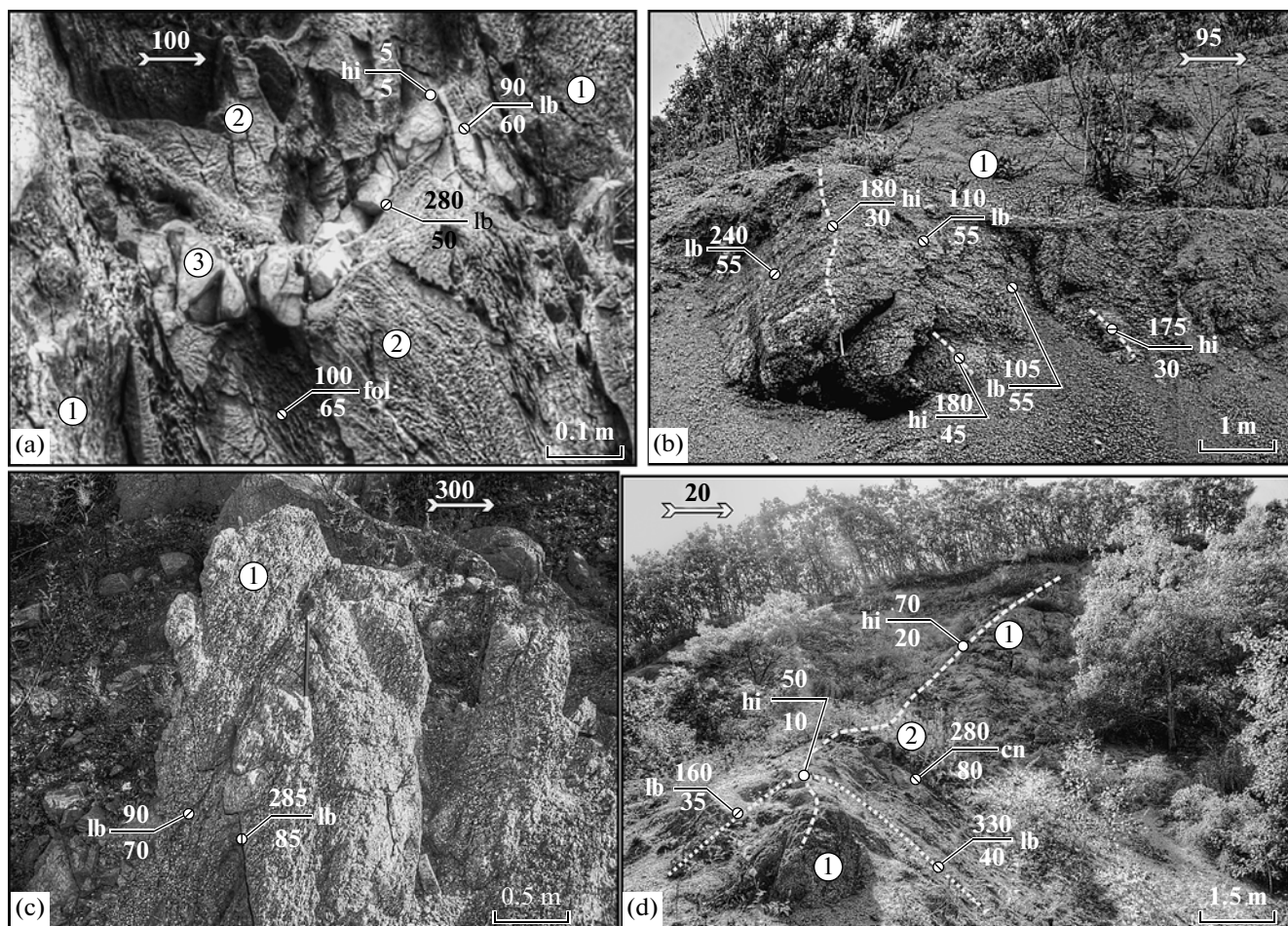
Fig. 8. Examples of shear pseudofolding and cleavage in the granites and metamorphic rocks.

(a) small shear fold consisting of aplite. Railway excavation near the settlement of Il'inka (see Fig. 2): (1) gneiss granite, (2) finely cleavaged metasedimentary rocks: siltstone and sandstone, (3) aplites. (b) shear fold in Vendian (?) granite gneiss (1). The fold was formed by conjugate shears represented by counter thrusts and then subjected to ductile deformations. Quarry in the right wall of the Nesterovka River. The assignment is shown in Fig. 2. (c) fine rhombic cleavage in granites (1) formed as a pure strike-slip-type conjugate shear by latitudinal compression; shear angle θ ≈ 60°. Shears split the rock and crystalline phenocrysts into small rhombs, thus providing a view of the cataclastic taxitic structure. Quarry on the left side of the Gryaznukha River (see Fig. 2). (d) quasi-fold of the Mesozoic fold−thrust warping of ENE trend in the meridionally sheared Permian granites. Numbers in circles: (1) gneiss granite, (2) andesite dike. A large dash denotes the fold hinge gently dipping to the east, while a small dash outlines the limbs of the quasi-fold. The quarry is located 4 km east of the settlement of Dvoryanka (see Fig. 2).

be noted that the crystal elongation is mainly subhorizontal and has a longitudinal direction, thus approximately coinciding with medium deformation axes σ_2^{PZ}, which were established by other features. Moreover, in many cases, regardless of the degree of gneissosity, one of three orthogonal cross sections (the plane *ac* (index according to B. Zander) or, in other words, the plane containing σ_1^{PZ} and σ_3^{PZ}) of Zander usually has a common granitic not gneissic structure. Thus, the coincidence of the linearities of the crystalline aggregates with the axis σ_2^{PZ}, which is marked by other structural elements, indicates the tectonic nature of the gneissosity. In addition, the gneissosity is often accompanied by synchronous cleavage (Fig. 7b),

which was formed by means of a pure strike-slip model. The conjugation lines of its fissures are concordant with the medium deformation axis σ_2^{PZ}.

The Mesozoic−Cenozoic geodynamic period is related to the regional compression σ_1^{MZ} of *NNW direction*. Such dynamic conditions correspond to the well studied sinistral strike-slip, which was typical of East Asia in the Mesozoic−Cenozoic [38]. The first-order elements were Triassic−Jurassic arches and troughs, and Cretaceous−Cenozoic coal-bearing depression of ENE strike. This period is subdivided into three episodes of compression activation: the Triassic−Jurassic, the Cretaceous, and the Tertiary, which are confirmed by reliable stratigraphic data. The strike-slip regime is peculiar in that each of the
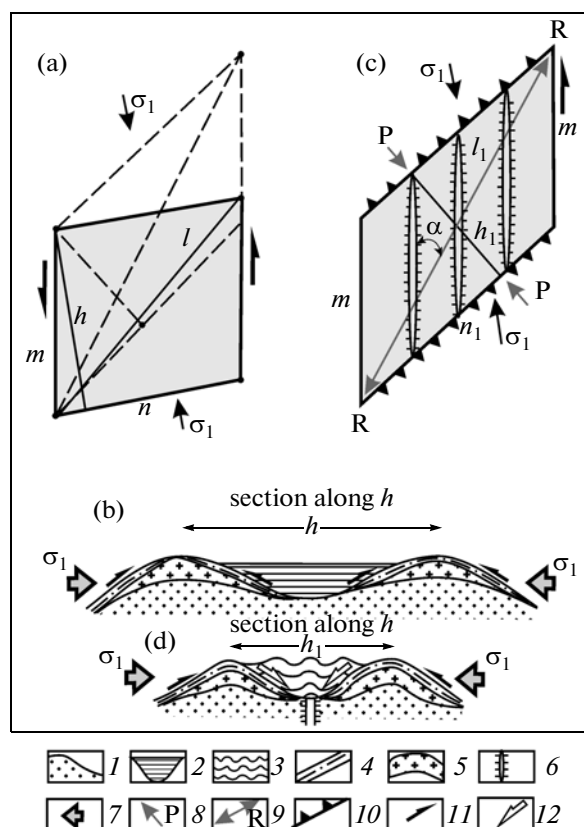
Fig. 9. Probable formation mechanism of the structure of the Mesozoic depressions under conditions of sinistral strike-slip. (a) and (c) in plan, (b) and (d) in section.

(a) m and n are the sides, h is the height, l is the long diagonal of the parallelogram that symbolizes the area of the basin's initiation. (b) section in profile h, the large and small arrows show the direction of the compression and thrusting, and the dashes denote the stratified complexes. (c) the same as in a but the parallelogram was formed by thrusting and strike-slipping; correspondingly, n, h, and l were deformed into n_1, h_1, and l_1. (d) section in profile h_1. (1) crystalline basement; (2) sedimentary deposits; (3) sedimentary sediments deformed by warping, (4) kinematic complexes; (5) arched areas of granitization; (6) fractures transformed into pull-aparts and normal faults; (7) direction of the main compression σ_1; (8) direction of warping (crust reduction) or their converging; (9) direction of extension; (10) thrusts in scheme b; (11) direction of thrusting in profile d; (12) inferred normal faults forming during the growth of the relief of the morphostructure.

three dynamic zones experienced two peaks of warping and strike-slipping. The role of the strike-slip dynamics in the episodes increases with the decreasing age of the tectonic events.

The beginning of *the Triassic–Jurassic episode* was dominated by warping. This resulted in the formation of alternating *antiform arches and synform troughs of the first order*, which at an acute angle cross early meridional structures extending ENE for 35–40 km at a width of 3–5 km (Fig. 2). These morphologies are well mappable because the troughs are filled with Triassic rhyolite–andesites, while the arches are made up of late Triassic and Early Jurassic granites. The volcanics in the troughs are deformed into longitudinal asymmetrical folds a few hundred meters wide. Their hinges dip gently (5–10°C) to the southwest. Warping is expressed by the dynamically similar processes of counter thrusting and folding. Typical folded forms were found in the hinge portions of the Paleozoic folds, i.e., in the areas where the Paleozoic beds have a gentle dip. In this case, the beds were deformed into folds of ENE extension as Mesozoic horizons. In the brittle metamorphic rocks, granites, and steep limbs of Paleozoic folds that are parallel to the direction of the Mesozoic–Cenozoic compression, warping was expressed by the shear paragenesis of counter thrusts with the subordinate role of folding. The "brittle warping" superposed onto the early structures can be exemplified by the small linear antiform observed in the road quarry near the settlement of Dvoryanka. This form as a sublatitudinal arch defined by conjugate counter thrusts is traced across the longitudinal foliation and gneissosity of Permian granites and basite (?) veins (Fig. 8d). Zones of large counter thrusts, which possibly participated in the formation of arches and troughs, are represented on the day surface by complexes ascribed to a single kinematic complex (Fig. 2). They are made up of the garnet–micaceous blastomylonite and mylonite, as well as chlorite and quartz–feldspar–sericite dynamoschist with single lenses of carbonates and siliceous rocks. The complex was deformed by numerous counter thrust detachments developed along the foliation and very obliquely cutting it. Idealized spatial relations of rocks developed in arches, troughs, and kinematic manifestations are shown in profiles h and h_1 (Fig. 9).

In addition to warping, the Triassic–Jurassic dynamic episode revealed a distinct peak of sinistral strike-slipping, which produced the paragenesis of strike-slips, pull-aparts, and normal faults. The NNW-trending pull-aparts ascribed to strike-slip paragenesis formed channels for the release of Triassic volcanic products. It is not occasional that the volcanic fields in the troughs contain numerous NW-trending rhyolite, dacite, and andesite extrusions, which are conformable to the strike-slip pull-apart basins. It is also logical that the extrusions are often rimmed by fractures with sinistral strike-slip and normal fault hatching. It is also noteworthy that these hatchings are discrete, although they were formed almost simultaneously. Both the hatchings are repeatedly rejuvenated in the same site and on the same surface.

A change of the warping by strike-slipping is also typical of the two subsequent episodes of tectonic activation: *the Early Cretaceous and Tertiary*. It is well expressed in the structure of the coal-bearing depressions.

The Early Cretaceous episode of the compression and warping activation clearly dominating at its beginning led to the formation of the Razdol'noe depression, which was filled with Barremian and Aptian–Albian coaliferous sandy–clayey deposits gently dipping to the SSE [12] and has an oval shape extended in the ENE direction. Strictly speaking, the depression as a morphstructure was initiated by compression as early as the Triassic and Jurassic, but it evolved more intensely in the Early Cretaceous.

3D mapping (Amel'chenko, 1995) showed that the Razdol'nensky basin consists of several synclines and anticlines of northern vergence, which were offset by SW-dipping strike-slip faults of the same vergence, along which Triassic rocks and Permian granites of the floor were thrust onto the accumulative Cretaceous deposits. The vergent folds and thrusts of the coal-bearing "bath" established by G.L. Amel'chenko were formed by warping directed frontally to the maximum compression. The subsequent strike-slip peak transformed the NS- and NW-trending faults into pull-aparts, which were partially intruded by granite porphyry dikes and converted into normal faults. This is consistent with the conclusions of V.V. Golozubov [12] concerning the mechanism of the basin formation.

At the same time, as was exemplified by the Cretaceous–Cenozoic Partizansky coal field [22], the indicated structural–kinematic pattern of the Razdol'noe depression could have been formed, in our opinion, by the impact of pervasive sinistral strike-slipping and the influence of NNW lateral compression.

In this context, it is reasonable to remember the model of suprastrike-slip folding proposed by G.V. Ryazanov [40]. According to this model, let us imagine the area of the basin initiation in the form of a parallelogram (Fig. 9). The sides of the parallelogram m and n represent the real tectonic elements: m designates the meridional sinistral strike-slips, while n denotes the ENE folds and thrusts (Fig. 9). Let them coincide with the contours of the depressions, which are marked by young stratified sediments. Let the area limited by the parallelogram be subjected to compression and sinistral strike-slip deformations (Figs. 9a, 9b). The parallelogram becomes longer under the sinistral strike-slip impact. The space toward the decreasing height of the areal figure ($h > h_1$) experiences the compression P to decrease with the formation of warping waves, which causes the appearance of arches and troughs. At the same time, the parallelogram is deformed by the compression of the long diagonal R: $l < l_1$. In other words, the early faults oriented at an acute angle to $l - l_1$ were opened and transformed into pull-aparts and normal faults (Figs. 9c, 9d). In order to compare the structuring of the Cretaceous Razdol'noe and Tertiary depressions, it is important to focus our attention on the fact that the wavy profile of the Razdol'noe depression floor is principally consistent with the fold asymmetry established by the prospecting, thus indicating the morphostructural–tectonic type of the floor topography. If this is the case, the floor's topography can be taken as a key kinematic indicator.

It is seen that the Razdol'noe depression is similar to the basins of the *Tertiary episode* in terms of the ENE orientation and asymmetrical structure of their bottom. Tertiary coal-bearing depressions (Pavlovka, Zharikovo, Turiy Rog, and Pogranichny) went through the same stages of the warping and strike-slipping under the impact of NNW compression. Note that the Pavlovka structure is located within the Razdol'noe depression and repeats all the morphological features of the latter. Fractures splitting depressions are dominated by normal faults. This implies that the Cretaceous and Tertiary depressions have no principal structural differences. Hence, the orientation of the maximum compression did not change and the dynamics of their formation can be explainable by the above proposed model (Fig. 9).

The mechanism of the superposition of warping and strike-slipping in each pulse remains unclear. Summing up the main points of the characteristics of the Cretaceous and Tertiary dynamic episodes, we may conclude that these deformations represent a dynamic and possibly asynchronous pair. In any case, using the structural control of the gold mineralization in the Sof'ye-Alekseevka area as an example (Fig. 5), we may suggest that thrust peaks are replaced by strike-slips also within short pulses. If this is the case, the "thrust–strike-slip" change is similar to the formation of conjugate shears. A significant point is that the conjugate shears are developed in a pulsed manner (not synchronously) alternating with small time intervals. Only conjugate systems in loose media are completely synchronous [36]. The nearly coeval manifestation of these phenomena, which is reflected in the structure of sufficiently large blocks, denotes that σ_2^{MZ} and σ_3^{MZ} alternated in space and time within local areas.

DISCUSSION

In addition to the orientation of the strain axes and the main structural–kinematic elements (Fig. 3f), an important factor directly affecting the structure of the region is the temporal structure of the loading activation or the character of the periodicity of the strain state. The general hierarchical series of activation pulses was determined: geodynamic period (first-order pulse) *dynamic episode (second-order pulse)* interval (third and 3 + n-order pulses). It was established that the axes of the medium and minimum strains change their orientation during long periods. During the *first* episode of the Proterozoic–Early Paleozoic geodynamic period, the thrust-fold structural paragenesis was developed in the crystalline basin in response to the main *meridional compression* σ_1^{PR}

with a low-angle axis and the medium compression σ_2^{PR} also having a low-angle but latitudinal axis. During *the second episode*, the vertical axis of the minimum strain σ_3^{PR} became low-angle and sublatitudinal, while σ_2^{PR} occupied a vertical position, although the maximum compression σ_1^{PR} remained the same. This stress transformation led to the disintegration and formation of the *en-echelon* structure of the basement. The Middle–Late Paleozoic period consists of two episodes, during which the maximum compression σ_1^{PZ} was latitudinal, while σ_2^{PZ} and σ_3^{PZ} were, respectively, sublongitudinal and vertical. During these episodes, the orientation of the main stress axes almost did not change. In contrast, in the *Mesozoic–Cenozoic period*, which is characterized in Sikhote Alin by the predominance of sinistral strike-slipping at the NNW-directed maximum compression axis σ_1^{MZ} [37], reorientations were recorded in each of the dynamic episodes distinguished within the period: the Triassic–Jurassic, Early Cretaceous, and Tertiary. The latter is subdivided into the Paleogene and Neogene intervals. The episodes and intervals, in turn, are subdivided into two and more pulses (see the previous section). Each episode involved the first warping pulse with horizontal σ_2^{MZ} and the second warping pulse with sinistral strike-slipping at vertical σ_2^{MZ}. In other words, depending on the predominance of warping or strike-slipping, the axes σ_2^{MZ} and σ_3^{MZ} alternated in a pulsed manner.

Our considerations concerning the periodic changing of the deformation mechanisms—fold–thrust–reverse faults by strike-slips, pull-aparts, and normal faults—are principally consistent with the conclusions of N.Yu. Vasil'ev and O.A. Mostryukov [5], which relate this phenomenon with a change in sign of the strains along the σ_1 axis. However, unlike these authors, we believe that a change in the regimes that mark the stages and phases of the evolution of the regional and local tectonic structures is related to the change of the strain signs toward the second and third main axis of the strain ellipsoid.

One of the main consequences of the pulsed evolution of the dynamic process is the warping deformation. The latter is essentially same as folding, which is mainly expressed by the development of counter shear thrusts, which caused the formation of secondary pseudofolds. Let us dwell on this widespread tectonic effect in more detail. It seems that these folds were initiated at the beginning of a pulse, in an impact way, in the initially isotropic medium and even across the strike of tightly compressed primary folding. It is reasonable that the limbs of the pseudofold initially had a planar shape, which is distinctly marked by aplites

(Fig. 6c). The latters additionally record the subsequent bending of these limbs up to the appearance of normal folds. The counter shear systems operate as the initial moment, which arranges the pseudofolds and causes the anisotropy of the isotropic medium. Therefore, granites are often deformed into pseudofolds. Such folds almost always overprint primary shadow structural elements and are "seemingly formed from a zero cycle" [26]. Convergent movements on the limbs of pseudoantiforms and divergent movements on the limbs of pseudosynforms make them similar with longitudinal folding [41] and differ them from folds of typical transverse compression and migmatite and cleavage shearing [20, 27, 33, 40]. While studying the structure of the Tafuinsky Massif (Fig. 1), we established not only shadow folds but also shear pseudofolds of two generations with orientation corresponding to the submeridional Cambrian compression, which was also recorded by this study in Western Primorye [25, 26]. This is also consistent with the refined geochronological age of the Tafuinsky Massif of 493 Ma, which corresponds to the Late Cambrian according to a new scale. The structure of the granitoid bodies in Western Primorye helped us to finally understand the mechanism of shearing pseudofolding, which was obtained during the study of the Tafuinsky and other massifs of Southern Primorye. Now, these concepts have received new confirmation and are discussed below.

Let the medium anisotropy be caused by the primary heterogeneity: the bedding or foliation of the granitized medium, S_0 (Fig. 10a). Assume that a pulse of tectonogenesis caused the compression strain σ_1, which gave birth to two main systems of conjugate shears of different polarity (S_1 and S_2) by means of pure strike-slip deformation (Figs. 10a, 10b, and 10c). Practically all the observed surfaces S_1 and S_2 are thrusts (Figs. 10d, 10e). Their combination served as a frame for the distribution of newly formed matter regardless of its genesis, for instance, most frequently aplites (Figs. 6d, 9c). One of the two conjugate shear systems usually is more developed than the other [36]. In our case, we observe the alternating predominance of S_1 or S_2, i.e., a system the shear movements along which are consistent with the systematic uprising movements along differently oriented $S0$ during longitudinal compression. The depressed shears are inferior to the dominant shears in length, frequency of manifestation, and (presumably) thrusting amplitude. As compared to the dominant shears, they are more often filled with magmatic material and are partially opened. In addition, this process is possibly accompanied by the formation of an extension zone (S_3), which is subparallel to the direction of the maximum compression in the plane $\sigma_1\sigma_2$. The opening of half-opened fractures sufficient for their aplitization occurs within this zone. Open shears marked by aplitization are transformed into pseudofolded veins and dikes
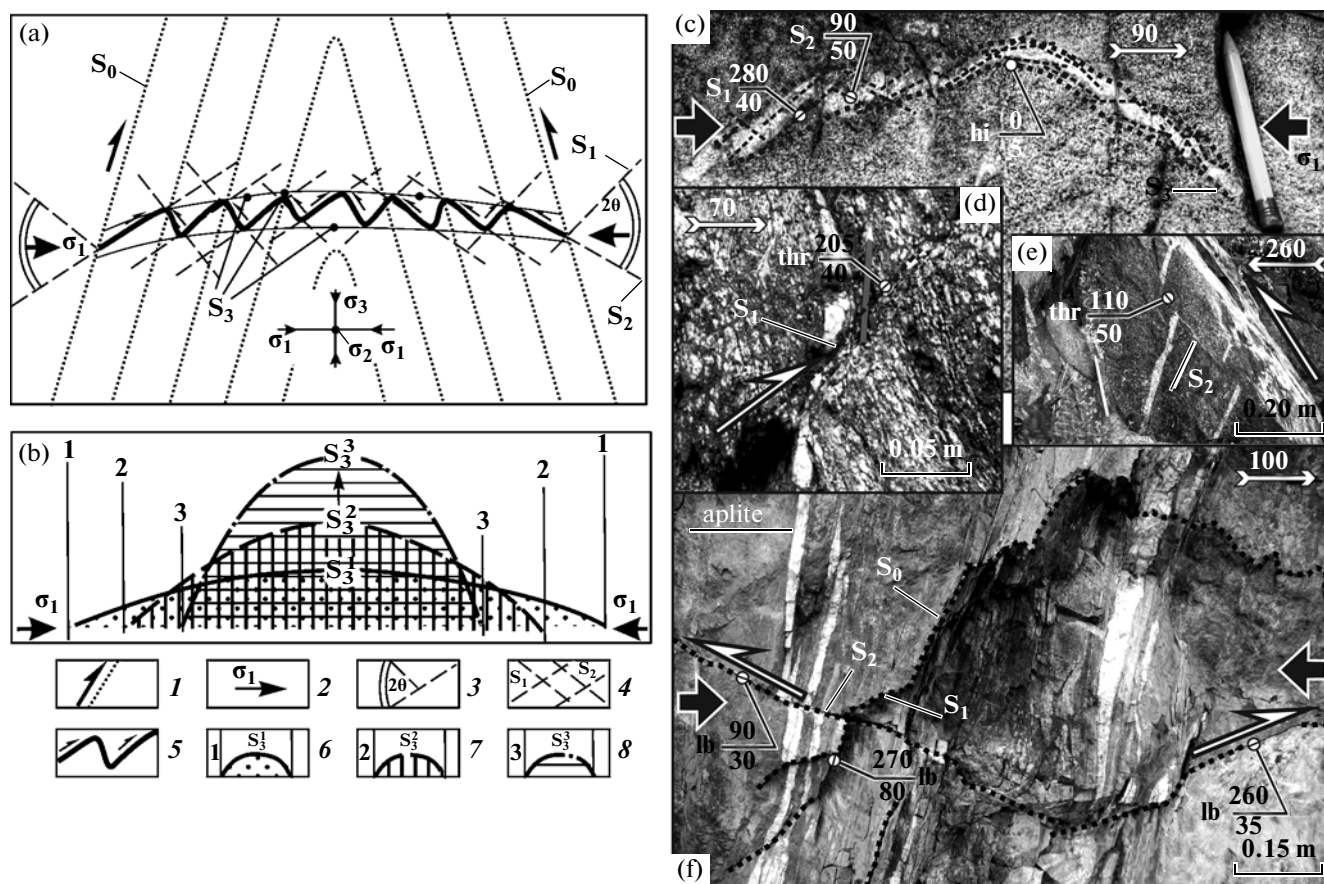
Fig. 10. Examples of the formation of secondary quasi-folded or pseudofolded forms by conjugate shears in the intrusive and metamorphic rocks and model scheme.

(a) formation of secondary conjugate shears and aplitization in their thinning zone (after [24, 25]); (b) possible staged bending of the shear-folded thinning zone.

(*1*) trajectory of foliation (S_0) of the idealized fold of the protoframework, the arrows show the predominant directions in the layer displacements; (*2*) direction of the main longitudinal compression; (*3*) the conjugation angle 2θ; (*4*) the conjugate shears (S_1 and S_2) formed by the longitudinal compression; (*5*) aplitized pseudofolded forms in the thinning zone bounded by surfaces (S_3); (*6*–*8*) the inferred bending of the S_3 zone with the subsequent arch formation during the three abstract compression pulses: (*6*) first, (*7*) second, (*8*) third. (c) shear-controlled aplites and the formation of pseudofolds. The assignment is shown in Fig. 2. (d) and (e) are examples of counter-dipping thrusts. (f) formation of the "virtual" unfilled shear quasi-folded antiform. The position is shown in Fig. 2a.

(Fig. 6). During the subsequent staged compression of the rock, zone S_3 is gradually bent occupying position $S_3^1 \longrightarrow S_3^2 \longrightarrow S_3^3$ (Fig. 10b). Bend S_3 is favorable for the growth of the porosity and microfissuring, which did not disturb the continuity of the rock. Foldlike forms often contain a series of conjugate unfilled shears (Fig. 10f). Based on the similarity between the small and large structural pseudofolds, we believe that their genesis is comparable with the mechanism of the formation of arches and troughs by means of crustal warping.

The Paleozoic and Mesozoic *granitization* of the rocks is possibly closely related to the formation of arches and smaller antiforms of the second and third orders. Granitiztaion is considered as a combination of processes that transform the solid rock of different origin in granites [2, 32]. The nature of granitization is thought to be different: related with magmatic replacement [2], metasomatism [17], and tectonics [32]. In the context of the obtained results, all these hypotheses seem quite reasonable but with allowance for the controlling role of external dynamics in the positioning and structuring of the intrusions. The fact that magmatic rocks are mainly accumulated in tectonically thinned arches casts no doubts [23, 24, 26]. In the geological maps of Primorsky Krai, most intrusions are concordant to the folding. According to the gravimetry, the intrusions are mainly low-angle and rootless. The granites from Southern and Western Primorye contain shadow textures that retain the orientation of the outer structural framework as well as pseud-

ofolds. The granitization is related to the enrichment of the rocks in alkalis and SiO_2 and the removal of Fe, Mg, and Ca and usually is developed at sufficiently deep depths, where it is accompanied by large-scale linearization of crystalline forms, thus forming a gneissosity of granites. This leads to the linearization of all the rock-forming minerals: quartz, feldspars, and hornblende. It is conceivable that, already at the cooling stage, the rocks become anisotropic, i.e., are capable of structuring under external pressure [29]. Thus, the gneissosity in the granites was produced by external tectonics, not by magmatic flowage. Such concepts concerning crystallization linearity and external compression were also reported by such known structural geologists as G.D. Azhgirei [1], E. Kloos et al. [15], W. Pitcher [28], and others. It is probable that this stage was responsible for the appearance of shear strains affecting the further structuring of granites [25, 26].

CONCLUSIONS

The analysis of the structural parageneses carried out for the first time in the Western Primorye region revealed three sequentially superposed structural patterns, which were formed, respectively, during the Late Proterozoic–Early Paleozoic, Middle–Late Paleozoic, and Mesozoic–Cenozoic geodynamic periods. Each of these periods was characterized by independent stress fields. The dynamics were characterized by a hierarchical pulsed structure. The different orientation of the axes and the pulsed manner of the outer dynamics led to the formation of the main morphostructural units, arches, and troughs, which resulted from the longitudinal crustal warping. It was established that warping occurred during each dynamic period and was implemented at different hierarchical levels from arches and troughs to small pseudofolds.

The warping and pseudofolding mechanism developed according to the example of the Tafuinsky Massif was confirmed in this work. In this work, we also confirmed the conclusions reached for the Uspensky, Tafuinsky, and other granitic massifs of Southern Primorye that the granite formation played a passive role, while the structures of the intrusions were mainly defined by the longitudinal lateral compression, since diapirism and transverse compression were not recognized. The combination of warping and strike-slipping peaks defined the morphology of the coal-bearing depressions during the Early Cretaceous and Tertiary episodes. The structuring mechanism proposed in this paper makes it possible to consider them as a result of warping against the background sinistral strike-slip regime.

The presented material shows that the geological evolution was controlled by the dynamic factor, although the structure formation, magmatism, and sedimentation were activated interactively. The study of the structuring dynamics provides insight into the structural arrangement of the region and the positioning of the tectonic elements ascribed to the different hierarchical ranks of the geological structure, including the terranes and complexes that join and overlie them. Direct tectonic studies allow the reconstruction of the regional and local structural evolution.

The established discrete and orthogonal changes in the orientation of the lateral compression presumably best correspond to the periodic acceleration and deceleration of the Earth's rotation, which was responsible for the change in the direction of the lateral displacements of the Asian continental and (or) Pacific plates from thrust to strike-slips and vice versa according to previously substantiated concepts [38, 39].

REFERENCES

1. G. D. Azhgirei, *Structural Geology* (MGU, Moscow, 1966) [in Russian].

2. A. Baddington, *Granite Emplacement with Special Reference to North America*, Bull. Geol. Soc. Am. **70**, 1959.

3. N. A. Belyaevskii, "Geological Zoning of USSR," in *Geological Structure of USSR. Volumes 1–3* (Gosgeoltekhizdat, Moscow, 1958), pp. 50–60 [in Russian].

4. I. I. Bersenev, "Western Primorye Structural Suture," in *Geological Problems of the Northwestern Sector of the Pacific Ore Belt* (Dal'nevost. fil. Akad. Nauk SSSR, Vladivostok, 1966), pp. 87–108 [in Russian].

5. N. Yu. Vasil'ev and A. O. Mostryukov, "Tectonophysical Reconstruction of the Localization Conditions of Noble Metals in the Dunites of the Layered Massif," in *M.V. Gzovskii and Development of Tectonophysics* (Nauka, Moscow, 2000), pp. 281–295 [in Russian].

6. N. P. Vasil'kovskii, *Paleogeology of Northeastern Asia* (Nauka, Moscow, 1984) [in Russian].

7. V. D. Voznesensky, "Structural Parageneses," in *Study of Tectonic Structures: Methodical Textbook on the Geological Survey on a Scale 1 : 50000* (Nedra, Leningrad, 1984), No. 16, pp. 84–101 [in Russian].

8. O. A. Votakh, *Structural Elements of the Earth* (Nauka, Novosibirsk, 1979) [in Russian].

9. *Geological Bodies: Terminological Reference Book*, Ed. by Yu. A. Kosygin, V. A. Kulyndyshev, and V. A. Solov'ev (Nedra, Moscow, 1986) [in Russian].

10. *The USSR Geology. Vol. 22. Primorsky Krai. Part 1. Geological Description* (Nedra, Moscow, 1969) [in Russian].

11. G. S. Gnibidenko, "Tectonics of the Khanka Massif," in *Materials on Tectonics and Petrology of the Pacific Ore Belt* (Nauka, Moscow, 1964), pp. 44−54 [in Russian].

12. V. V. Golozubov, *Tectonics of the Jurassic and Lower Cretaceous Complexes in the Northwestern Pacific Framing* (Dal'nauka, Vladivostok, 2006) [in Russian].

13. L. F. Nazarenko and V. A. Bazhanov, "Main Features of Tectonics and Evolution," in *Geology of Primorsky Krai* Preprint. Part 3 (DVGI DVO AN SSSR, Vladivostok, 1989) [in Russian].

14. L. A. Izosov, *Problems of Geology and Diamond Potential of the Continent−Ocean Transition Zone (Seas of Japan and Okhotsk Regions)* (Dal'nauka, Vladivostok, 2006) [in Russian].

15. E. Kloos, F. Turner, D. Griggs, et al., "Problems of Structural Geology," (Izd-vo inostr. lit-ry, Moscow, 1958) [in Russian].

16. L. I. Krasnyi, A. S. Vol'skii, Pen Yun'byao et al., *Geological Map of the Amur Region and Adjacent Areas. 1 : 2500000. Explanatory Notes* (Kharbin−Blagoveshchensk, St. Petersburg, 1999) [in Russian].

17. Yu. A. Kudinov, *Metasomatism as a Leading Process in the Earth's Crust Evolution* (GEOS, Moscow, 2003) [in Russian].

18. R. G. Kulinich, Extended Abstracts of Candidate's Dissertation in Geology and Mineralogy (Vladivostok, 1969).

19. Yu. S. Lipkin, "Some features of Structure of the Khanka Massif and History of Its Evolution," in *Geological Problems of the Northwestern Pacific* (Dal'nauka, Vladivostok, 1966) [in Russian].

20. Luk'yanov, A.V., *Ductile Deformations and Tectonic Flowage in the Lithosphere* (Nauka, Moscow, 1991).

21. M. A. Mishkin, Chzhao Chuitszin, E. P. Lelikov, et al., "Precambrian Khanka and Jiamusi Median Massifs. Stratigraphic Correlation," Tikhookean. Geol., No. 6, 85−95 (1993).

22. P. L. Nevolin, "Stages and Mechanisms of Structural Formation of the Partizansky Coal Basin, Southern Primorye," in *Regularities in Structure and Evolution of Geospheres. Proceedings of 3rd International Interdisciplinary Symposium, Khabarovsk, Russia, 1998* (Priamur. geogr. ob-vo, Khabarovsk, 1998), pp. 246−248 [in Russian].

23. P. L. Nevolin, V. P. Utkin, A. N. Mitrokhin, et al., "Cretaceous Intrusions of the Southern Primorye: Tectonic Position, Structure, and Dynamics of their Formation," Tikhookean. Geol. **22** (5), 73−86 (2003).

24. P. L. Nevolin, V. P. Utkin, T. K. Kutub-Zade, et al., "Geodynamics of Structuring and Metallogenic Aspects of the Northern Part of Western Primorye," in *Pacific Ore Belt: Materials of New Studies* (Dal'nauka, Vladivostok, 2008), pp. 278−298 [in Russian].

25. P. L. Nevolin, V. P. Utkin, and A. N. Mitrokhin, "Pseudofolded Control of Aplite Dikes in the Paleozoic Intrusions of Southern Primorye," in *Tectonics and Geodynamics of the Phanerozoic Folded Belts and Platforms: Proceedings of 43rd Tectonic Conference* (GEOS, Moscow, 2010), Vol. 2, pp. 81−85 [in Russian].

26. P. L. Nevolin, V. P. Utkin, and A. N. Mitrokhin, "The Tafuinsky Granite Massif, Southern Primorye Region: The Structures and Geodynamics of Longitudinal Compression," Russ. J. Pac. Geol. **4** (4), 331−346 (2010).

27. E. I. Patalakha, *Genetic Principles of Morphological Tectonics* (Nauka, Alma-Ata, 1981) [in Russian].

28. W. Pitcher, "Ghost Stratigraphy in the Intrusive Granites: a Review," Geol. J. **2**, 123−140 (1970).

29. M. Reiner, *Geology* (Nauka, Moscow, 1965) [in Russian].

30. L. M. Rastsvetaev, "Some Common Models of Disjunctive Fracture Deformations," in *Experimental Tectonics in the Theoretical and Applied Geology* (Nauka, Moscow, 1985), pp. 118−126 [in Russian].

31. A. M. Smirnov, *Juncture of the Chinese Platform with Pacific Fold Belt* (AN SSSR, Moscow, 1963) [in Russian].

32. E. P. Smirnov, "Role of Magmatic Replacement during Formation of the Transural Granitoids," Dokl. Akad. Nauk SSSR **218** (2), 442−445 (1974).

33. E. W. Spencer, *Introduction to the Structure of the Earth* (McGraw-Hill, New York, 1977) [in Russian].

34. A. I. Khanchuk, Extended Abstracts of Doctoral Dissertation in Geology and Mineralogy (Geol. Inst., Moscow, 1993).

35. A. I. Khanchuk, V. V. Ratkin, M. D. Ryazantseva, et al., *Geology and Minerals of the Primorsky Krai: a Review* (Dal'nauka, Vladivostok, 1995) [in Russian].

36. S. I. Sherman, S. A. Bornyakov, and V. F. Buddo, *Zones of Dynamic Fault Influence: Modeling Results* (Nauka, Novosibirsk, 1983) [in Russian].

37. Sherman, S.I. and Dneprovskii, Yu.I., *Strain Fields of the Earth's Crust and Geological−Structural Methods of Their Study)* (Nauka, Novosibirsk, 1989).

38. V. P. Utkin, "Reversible Transformation of the Nappe-and-Thrusts and Strike-Slip Dislocations," Dokl. Akad. Nauk SSSR **249** (2), 425−429 (1979).

39. V. P. Utkin, P. L. Nevolin, and A. N. Mitrokhin, " Late Paleozoic and Mesozoic Deformations in the Southwestern Primorye Region," Russ. J. Pac. Geol. **1** (4), 307−323 (2007).

40. V. Yaroshevsky, *Fault and Fold Tectonics* (Nedra, Moscow, 1981) [in Russian].

41. H. Ramberg, "Evolution of Drag Fold," Geol. Mag. **100** (2), 97−106 (1963).

Recommended for publishing by A.I. Khanchuk